Ice-shelf elevation changes due to atmospheric pressure variations

Laurie PADMAN,[1] Matt KING,[2] Derek GORING,[3]* Hugh CORR,[4] Richard COLEMAN[5,6,7]

[1]*Earth & Space Research, 3350 SW Cascade Ave., Corvallis, Oregon 97333-1536, U.S.A.*
E-mail: padman@esr.org
[2]*School of Civil Engineering and Geosciences, Bedson Building, University of Newcastle upon Tyne, Newcastle upon Tyne NE1 7RU, England*
[3]*National Institute of Water and Atmospheric Research Ltd, Box 8602, Christchurch, New Zealand*
[4]*British Antarctic Survey, Natural Environment Research Council, Madingley Road, Cambridge CB3 0ET, England*
[5]*School of Geography and Environmental Studies, University of Tasmania, Private Bag 78, Hobart, Tasmania 7001, Australia*
[6]*CSIRO Marine Research, Box 1538, Hobart, Tasmania 7001, Australia*
[7]*Antarctic CRC, University of Tasmania, Private Bag 80, Hobart, Tasmania 7001, Australia*

ABSTRACT. The inverse barometer effect (IBE) is the isostatic response of ocean surface height to changes in atmospheric pressure (P_{air}) at a rate of about $1\,\mathrm{cm\,hPa^{-1}}$. The IBE is a significant contributor to variability of ice-shelf surface elevation (η_{ice}), as we demonstrate with simultaneous global positioning system measurements of η_{ice} and local measurements of P_{air} from the Amery, Brunt and Ross Ice Shelves, Antarctica. We find that an IBE correction is justified for frequencies (ω) covering the "weather band", $0.03 < \omega < 0.5$ cpd (cycles per day). The IBE correction reduces the standard deviation of the weather-band signal of η_{ice} from ~9 cm to ~3 cm. With this correction, the largest remaining high-frequency error signal in η_{ice} is the inaccuracy of the present generation of Antarctic tide models, estimated to be of order 10 cm for most of Antarctica.

INTRODUCTION

In this paper we discuss ice-shelf surface elevation (η_{ice}) changes associated with varying atmospheric pressure (P_{air}). On sufficiently long time-scales and away from coastal effects, the ocean's isostatic response is ~1 cm depression of sea level for a 1 hPa increase in P_{air} (Gill, 1982; Ponte and others, 1991; Ponte, 1993). This ideal response is known as the inverse barometer effect (IBE). The IBE is a well-known signal in sea surface height (SSH) that is routinely removed before interpreting open-ocean height variability sensed by satellite radar altimeters (see, e.g., Chelton and Enfield, 1986). The IBE correction is not yet, however, routinely applied when processing altimetry or synthetic aperture radar (SAR) data acquired over ice shelves. In this paper, we use precision global positioning system (GPS) measurements from several large Antarctic ice shelves to demonstrate that the IBE correction should be made when processing remote-sensing data for ice shelves, particularly when measuring lateral flow rates with SAR interferometry (InSAR) based on image pairs with short time separation. We also identify the magnitude of the errors that arise through the difference between the ideal IBE response and the true response of the ocean and ice shelves to changes in P_{air}.

The IBE implies that, for a typical change of ~40 hPa in P_{air} during passage of an energetic polar low, there will be a ~40 cm change in η_{ice} for freely floating portions of ice shelves. This value is generally less than the daily range of η_{ice} due to tides, which frequently exceeds 2 m and can exceed 7 m (Fricker and Padman, 2002; Padman and others, 2002), but is larger than the typical error of order 10 cm for present-generation Antarctic tide models (Padman and others, 2002, 2003). The tidal contribution to high-frequency variability of η_{ice} is always removed prior to analyses of altimetry and InSAR, so the IBE would be the largest high-frequency signal remaining in η_{ice}.

The question we need to address, however, is: To what extent is the IBE approximation valid around Antarctica? Ponte and others (1991) used atmospheric pressure forcing in barotropic numerical models of large ocean basins to investigate the response of the deep ocean to P_{air} as a function of temporal and spatial scales of P_{air} variability. They found that the isostatic approximation (the IBE) was generally valid for time-scales longer than ~1 week, although Ponte (1993) described additional studies suggesting that the IBE approximation at these time-scales was poor in some geographical areas, notably including the Southern Ocean. At periods of ~2 days, the true response to P_{air} variability deviated from the IBE by ~20% in a globally averaged sense. At short time-scales and especially in the shallower seas close to coasts where other processes such as wind set-up and coastal trapped waves may be important, the IBE is not expected to be a good model of sea-level response. From this discussion we should not be surprised if the IBE turns out to be a poor predictor of sea level and η_{ice} variability around Antarctica.

We are only aware of three publications that explore the relationship between sea level or η_{ice} variability and P_{air} near Antarctica. Potter and others (1985) found a residual

---

* Present address: Mulgor Consulting Ltd, 24 Brockworth Place, Riccarton, Christchurch, New Zealand

signal in sea level sensed by a bottom pressure recorder near the Eklund Islands in George VI Sound of about 10 cm peak-to-peak (their fig. 4): the magnitude of this signal is about 35% of the IBE response. These authors acknowledge, however, that unresolved long-period (fortnightly and monthly) tides may contribute to the observed sea-level signal in their short record. Rignot and others (2000) used the IBE to explain small discrepancies between tidal variability sensed with differential InSAR and model predictions for sections of ice shelf along the Ronne and Filchner Ice Shelf fronts. The expected IBE-induced signal was consistent with the errors between models and data, but the magnitude of the IBE signals was similar to the tidal model uncertainty. A recent analysis of sea-level (coastal tide-gauge) data from Ross Island and Cape Roberts in the Ross Sea (Goring and Pyne, 2003) indicates that, after tides are removed, the IBE is the largest signal in SSH adjacent to the Ross Ice Shelf. The "barometric factor", the ratio of the measured response of η_{ice} to the IBE, varied in that study from about 0.80 to 1.06 over a range of time-scales, but with a mean of ~0.90. That is, a simple IBE correction accounted for ~90% of the total coherent response of sea level to P_{air}. The authors proposed that the validity of the IBE in this coastal dataset is due to the generally weak winds in this region of the southwestern Ross Sea.

In the present paper, we seek further evidence of the reliability of the IBE in Antarctica through analyses of simultaneous in situ measurements of η_{ice} and P_{air} from three widely separated ice shelves. We identify the frequency range over which the IBE is a reasonable correction, demonstrate the importance of the IBE correction for satellite measurements of ice-shelf motion and calculate the typical error in estimates of η_{ice} resulting from deviations of $\eta_{ice}(P_{air})$ from the ideal IBE.

DATA

The principal datasets for our study are GPS measurements of η_{ice} variability on the Amery, Brunt and Ross Ice Shelves, and simultaneous records of P_{air} (Table 1). The GPS measurements were processed using the Precise Point Positioning (PPP) strategy (Zumberge and others, 1997), estimating the three-dimensional coordinates of the antenna and tropospheric zenith delays every 5 min (King and Aoki, 2003). The data were processed in 30 hour batches and then truncated to the central 24 hours to avoid filter-edge effects. The station motion and the variation of the tropospheric zenith delay were both modeled as random-walk stochastic processes. We tuned the station coordinate random-walk standard deviation σ_{rw} at each site to ensure that the site motion was neither over-constrained, hence minimizing damping of the tidal signal, nor under-constrained, hence removing unnecessary noise from the solutions. The σ_{rw} values adopted were 48 mm h$^{-0.5}$ for the Amery Ice Shelf sites, 60 mm h$^{-0.5}$ for the Ross Ice Shelf site and 480 mm h$^{-0.5}$ for the Brunt Ice Shelf site. The significantly higher value for the Brunt Ice Shelf is due to the much larger tidal range at this site. For the tropospheric zenith delay, we adopted a σ_{rw} of 4.8 mm h$^{-0.5}$. Since the PPP technique is sensitive to the absolute motion of the earth's surface, we modeled solid-earth and pole tides at this stage. The effect of ocean loading was removed from the GPS time series during the harmonic analysis described below. Other load-

Table 1. Total variance of detrended η_{ice} ($\sigma^2(\eta_{ice})$); tidal band, $0.85 < \omega < 2.1$ cpd ($\sigma^2(\eta_{Tide})$); residual after tide removed ($\sigma^2(\eta')$); weather band, $0.03 < \omega < 0.5$ cpd ($\sigma^2(\eta_{WB})$); weather band P_{air} ($\sigma^2(P_{air})$); weather band after IBE correction ($\sigma^2(\eta'_{WB})$); and tidal band after removal of tides through analysis of time series as described in text ($\sigma^2(\eta'_{Tide})$). All values are in cm^2. The bottom two rows are the slope of the linear least-squares fit between weather-band P_{air} and η (Slope) and the correlation coefficient for this fit (r)

	BIS		*AIS*		*Ross Island*	*RIS*
	Halley	*TS-01*	*TS-03*	*TS-04*	*Scott Base*	*WFLDBF*
Record length	763.0	48.5	59.5	64.6	470.0	31.0
$\sigma^2(\eta_{ice})$	4691	1520	1449	1622	733	628
$\sigma^2(\eta_{Tide})$	4493	1412	1331	1509	636	568
$\sigma^2(\eta')$	98	108	118	113	97	60
$\sigma^2(\eta_{WB})$	61	78	86	88	59	29
$\sigma^2(P_{air})$	58	82	73	71	48	28
$\sigma^2(\eta_{WB})$	10	8	16	12	15	11
$\sigma^2(\eta_{Tide})$	7	16	26	34	2	8
Slope	0.94	0.93	0.98	1.04	0.96	0.82
r	0.92	0.95	0.90	0.93	0.87	0.80

Notes: The six stations are Halley on the Brunt Ice Shelf (BIS), TS-01, TS-03 and TS-04, all on the Amery Ice Shelf (AIS); the coastal tide gauge at Scott Base on Ross Island and the Williams Field Long Duration Balloon Facility (WFLDBF) near McMurdo Base on the Ross Ice Shelf (RIS).

ing signals, such as atmospheric loading, with expected total magnitudes of ~1–2 cm, remain in the GPS time series.

For each GPS record, corresponding pressure data were obtained. For the Amery, these were collocated with the GPS measurements and have a precision of ~0.7 hPa. The pressure measurements for the other sites were obtained using more precise equipment, and these measurements may be regarded as error-free for our purposes.

In addition, we looked at coastal SSH data recorded at Scott Base (on Ross Island) and Cape Roberts in the Ross Sea near the western end of the Ross Ice Shelf front, as previously reported by Goring and Pyne (2003). The Scott Base recorder is a nitrogen bubbler system attached to the reverse osmosis boom. The heat from the reverse osmosis pipe ensures there is always a hole in the ice, even in winter. Sea-level data and atmospheric pressures are recorded every 5 min and telemetered to Christchurch, New Zealand, every day where they are checked and archived. The Cape Roberts recorder is a vented pressure transducer that also records at 5 min intervals. The data are recovered periodically when the site is visited. The data used in this study came from the period 17 January 2001 to 3 May 2002, a total of 471 days. The Ross Island data are gap-free, but the Cape Roberts data have gaps of several days in February and November 2001.

The tidal height signal (η_{Tide}) was removed from each time series of η_{ice} and SSH using Matlab^{TM} software (Pawlowicz and others, 2002) based on the algorithms developed by Foreman (1977). Each time series of the residual $\eta'(t) = \eta_{ice}(t) - \langle \eta_{ice} \rangle - \eta_{Tide}(t)$ (where $\langle \eta_{ice} \rangle$ is the record-length time average of η_{ice}) consists of the response to P_{air}, tidal-band energy that is not fitted, other non-tidal contributions to η_{ice}, and measurement noise. For reasons that will be explained below, we define the range of frequencies (ω)
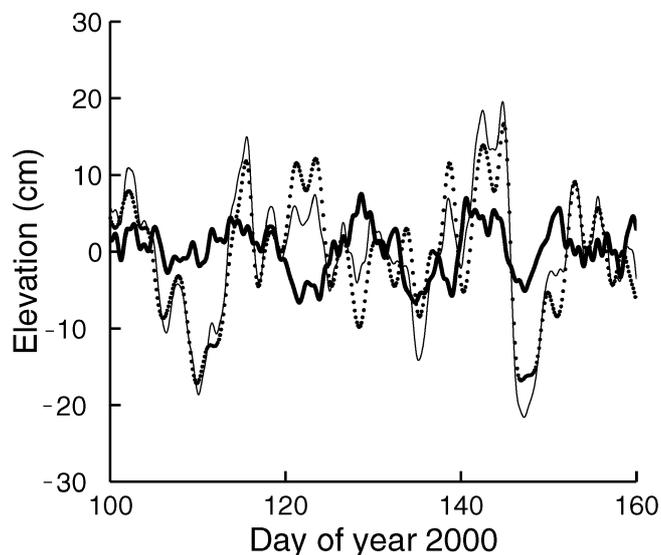
Fig. 1. Time series of bandpassed (0.03 < ω < 0.5 cpd) ice-shelf surface height anomaly η_WB (thin solid line), ideal IBE −1.01 P_air (dotted line) and weather-band residual η_WB (thick solid line) for Halley Base on the Brunt Ice Shelf. Sixty days of data from 2000 are shown.

between 0.03 and 0.5 cycles per day (cpd) as the "weather band". Figure 1 shows a section of weather-band variability in the GPS and air-pressure records at Halley Base on the Brunt Ice Shelf. We see that reasonable agreement between η' and $-P_{air}$ occurs through most of this time series.

RESULTS

In this section, we first review analyses of data from our longest ice-shelf GPS record from Halley Base on the Brunt Ice Shelf, then analyses of three GPS stations from the Amery Ice Shelf. Ocean SSH data from coastal tide gauges in the western Ross Sea are then reviewed, and compared with GPS data from a nearby GPS site on the Ross Ice Shelf.

Brunt Ice Shelf

The longest ice-shelf GPS time series we have is the 763 day record (beginning 5 January 1999) from Halley Base on the Brunt Ice Shelf, which therefore warrants the most detailed analysis in this paper. The Halley data and processing techniques are described by Doake and others (2002). About 10% of this record is bad or missing data: for the purposes of further time-series analysis, gaps have been padded with computed values based on the ideal IBE values added to the predicted tide derived from analyses of the good data. The power-density spectra for η' and P_{air}, $\Psi(\eta')$ and $\Psi(P_{air})$, respectively, for the Halley time series (Fig. 2) show that amplitudes for both spectra are similar for frequencies $\omega < 0.5$ cpd. For $\omega > 0.5$ cpd, energy in $\Psi(P_{air})$ falls rapidly with increasing ω. The spectrum of η' contains some energy in the principal tidal bands centered on 1 and 2 cpd, with additional energy at higher tidal harmonics. Recall that the time series of η' is already detided, and that detiding was performed with analysis of $\eta_{ice}(t)$, not by an independent tide model. This residual tidal energy is associated with additional minor tidal harmonics and spreading of the main tidal lines by non-linear interactions with other ocean phenomena and the ice shelf itself. The squared coherence of
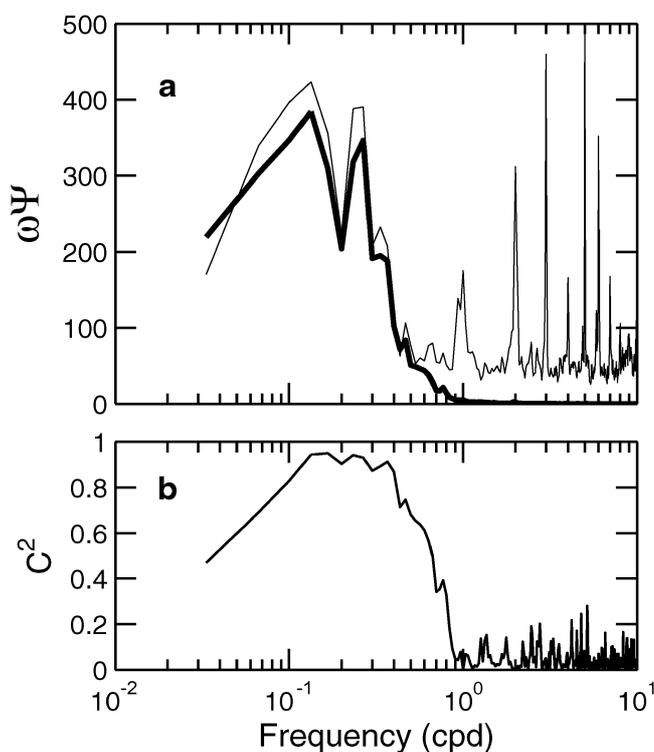

Fig. 2. (a) Area-preserving spectra (frequency ω times spectral density Ψ) of P_air (thick line) and detided ice-shelf surface elevation anomaly (η′; thin line) for the entire record from Halley Base on the Brunt Ice Shelf. See text for detiding procedure and explanation for remaining tidal-band energy. (b) Squared coherence (C²) for the spectra in (a). C² falls to 0.5 at ∼0.03 and ∼0.5 cpd, defining the weather band.

the spectra $C^2(\omega)$ for the Halley measurements (Fig. 2) was > 0.8 for $0.1 < \omega < 0.4$ cpd, falling to 0.5 near 0.03 and 0.5 cpd. We define the band $0.03 < \omega < 0.5$ cpd as the weather band since this band contains most of the variance in P_{air}. At higher frequencies, tides and measurement noise dominate η', and at lower frequencies some of the variability of η' is expected to arise from seasonal and climatological changes in the ice thickness and systematic motion of the GPS antenna, and in the underlying ocean state.

The variances for different stages in data processing are listed in Table 1. The variance of the total ice-shelf height signal is $\sigma^2(\eta_{ice}) = 4691$ cm^2. The tide fit as discussed above captures $\sim 96\%$ of the total variance ($\sigma^2(\eta_{tide}) = 4493$ cm^2). The residual signal in the weather band after the optimum IBE correction is made, η'_{WB}, has a variance of $\sigma^2(\eta'_{WB}) \approx 10$ cm^2, which is comparable to the residual tidal-band variance of $\sigma^2(\eta_{tide}) \approx 7$ cm^2. From the 60 day record shown in Figure 1, we see that the magnitude of (η'_{WB}) occasionally exceeds 10 cm, so that future studies will need to determine the source of (η'_{WB}).

The least-squares linear fit between weather-band η' (denoted η'_{WB}) and P_{air} is

$$\eta_{WB} \approx -0.94 P_{air}, \qquad (1)$$

with a correlation coefficient of $r \approx 0.92$. The constant 0.94 in Expression (1) is $\sim 7\%$ less than the expected value from the assumption of isostasy, but is slightly larger than the value found from coastal tide gauges in the Ross Sea (Goring and Pyne, 2003).

Amery Ice Shelf

Three Amery GPS records were chosen for analysis, varying in length from 48.5 to 64.6 days (Table 1). The value of $\sigma^2(\eta_{\mathrm{WB}})$ is slightly higher than for the Halley record, averaging $\sim$84 cm^2 for the three stations. After the standard IBE correction is made, $\sigma^2(\eta'_{\mathrm{WB}}) \approx 12$ cm^2 and $\sigma^2(\eta_{\mathrm{Tide}}) \approx 25$ cm^2. The latter value is $\sim$3.5 times the magnitude of $\sigma^2(\eta_{\mathrm{Tide}})$ for the Halley data, even though the variance of the fitted tide to Amery data is about one-third of the same value for Halley. This result reflects the effect of shorter records on tidal analyses: 68 tidal constituents are evaluated for the long record at Halley, while only 35 are evaluated for the shorter Amery records and with a larger error on each constituent.

The mean slope for the three Amery stations indicates an optimum correction for atmospheric effects of $\eta_{\mathrm{WB}} \approx -0.98 P_{\mathrm{air}}$ ($r \approx 0.93$) compared with $-0.94 P_{\mathrm{air}}$ for Halley.

Ross Sea coastal tide gauges

Goring and Pyne (2003) applied wavelet analyses to investigate the response of the Ross Sea sea level to changing P_{air}. Wavelet analysis allows the signal to be split into components of various time-scales such that the response can be analyzed independently at each time-scale. For time-scales between 32 and 256 hours, i.e. roughly the same time-scales identified by Fourier analysis as high coherence in the Brunt Ice Shelf data, there is an almost direct response of sea level to atmospheric pressure changes. The response was weaker at longer time-scales. The proportion of the variance in detided sea level that could be explained by atmospheric pressure was 71% over all time-scales, but had a maximum of 83% at 64 hour time-scales. These proportions are higher than normal for coastal sites and indicate the relative absence of wind effects on sea level in the Ross Sea.

For direct comparison with the ice-shelf GPS studies, we analyze the long Scott Base (Ross Island) record in the same manner as for the Brunt and Amery GPS sites. The western side of the Ross Sea has small tides (Padman and others, 2003), and this is seen in the reduced total and tide-band variance at Scott Base relative to the other sites (see Table 1). The weather-band variance of P_{air} is also smaller, and this is reflected in $\sigma^2(\eta_{\mathrm{WB}})$. The linear least-squares approximation of the weather-band response is $\eta_{\mathrm{WB}} \approx -0.96 P_{\mathrm{air}}$ ($r \approx 0.87$). The residual tidal-band variance for this record is only 2 cm^2, an order of magnitude smaller than for the GPS records. Part of the reduction will be due to the higher accuracy of the coastal tide-gauge record compared with GPS and the longer record allowing fitting of more tidal harmonics to the time series. We also note, however, that this tide-gauge record only contains higher tidal harmonic energy near 4 cpd, whereas the longest ice-shelf GPS record (Brunt) contains energy at all harmonics above 2 cpd (Fig. 2). This result suggests that there are non-linear responses of the Brunt Ice Shelf to ocean tides, possibly associated with grounding-line migration through a tidal cycle or cyclic changes in internal ice stresses, which are not present in ocean sea-level fluctuations.

Ross Ice Shelf

One month's GPS data were collected at the Williams Field Long Duration Balloon Facility near McMurdo Base on the Ross Ice Shelf, in support of the RADARSAT ground-con-
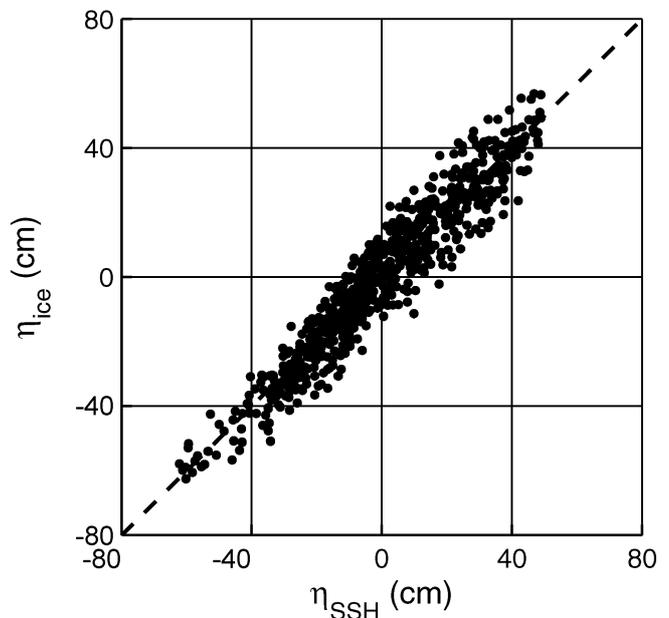

Fig. 3. Comparison of Cape Roberts coastal tide gauge (η_{SSH}) and Ross Ice Shelf GPS (η_{ice}) for a 31 day period in 1999. The diagonal dashed line indicates equivalence between the records. The similarity of the two records indicates that our fundamental assumption of the ice shelf's isostatic response to changing SSH is correct.

trol project in late 1999. Table 1 shows the variances for this record. A comparison of the elevation data for this record with the nearby coastal tide gauge at Cape Roberts (Fig. 3) indicates that the ice shelf is responding isostatically to the ocean SSH variability (see also King and Aoki, 2002). The reduced weather-band variance of height, $\sigma^2(\eta_{\mathrm{WB}})$, compared with the Scott Base coastal tide-gauge data (Table 1), is simply due to the small value of $\sigma^2(P_{\mathrm{air}})$ during the 31 days that GPS data were collected on the ice shelf.

The linear least-squares approximation to the weather-band response to P_{air} changes is $\eta_{\mathrm{WB}} \approx -0.82 P_{\mathrm{air}}$ ($r \approx 0.80$). This record has a much larger deviation of the IBE from the theoretical value than any other record. We attribute this result to the short record length and to the low variance of P_{air} for the 1 month period, so that measurement noise in the GPS record is a larger fraction of the weather-band variability of η_{ice}.

DISCUSSION AND CONCLUSIONS

The IBE is the main component of weather-band ($0.03 < \omega < 0.5$ cpd) variability of ice-shelf surface height η_{ice}. The standard deviation of weather-band variability of η_{ice} due to the IBE at the ice-shelf sites that we analyzed is $\sim$8–10 cm. For the two longest records, 763 days of GPS at Halley Base on the Brunt Ice Shelf and 470 days of coastal sea level at Scott Base on Ross Island, the empirically determined slope of the linear least-squares fit between weather-band η_{ice} and P_{air} is -0.95 ± 0.01 cm hPa^{-1}. This value is $\sim$6% less than the theoretical IBE value of $\sim$$-1.01$ cm hPa^{-1}, which is consistent with deformation of the solid earth by the increased atmospheric loading, comparable to ocean tidal loading (Ray and Sanchez, 1989). Even ignoring this effect, the difference between the empirical weather-band corrections and the IBE amounts to only order 1 cm^2 vari-

ance, which is much less than the residual variance in the weather band after the optimum IBE correction is made ($\sim$10 cm^2), and is also smaller than the residual signal in the tidal frequency band after the optimum tidal fit to the data is removed. We conclude that the theoretical IBE, perhaps with a small atmospheric loading correction, should be applied routinely to satellite SAR and altimetry data at the same time as tidal corrections are made.

In practical terms, the principal limitation to the quality of the IBE correction is not the accuracy of the correction itself, but rather the quality of the "measurement" of P_{air}. All the sites we analyzed in this study are close to weather stations that report in real time to global atmospheric models, so that the records of P_{air} from model outputs closely match the data used here. In more remote regions, such as the interior of the Filchner–Ronne Ice Shelf in the southern Weddell Sea, air pressure may be poorly represented by the models. As D. Bromwich (personal communication, 2002) has noted, the problem is not solely one of adequately modeling the intensity of pressure systems but also of accurately predicting the time of passage of weather fronts, during which P_{air} may change by 40 hPa or more (see near $t = 145$ in Fig. 1). A slight error in timing the passage of such fronts can lead to a misinterpretation of satellite-derived ice-shelf height variability, even though the basic mechanism of the IBE is appropriate.

The most important application of improved corrections to η_{ice} is the processing of repeat-pass remote-sensing measurements (e.g. InSAR) to estimate ice-shelf horizontal velocities (see, e.g., Rignot and MacAyeal, 1998). The contribution of vertical displacement to estimates of lateral velocity occurs because the SAR look angle is not vertical: for the European Remote-sensing Satellite (ERS), the angle is $\sim$23°. The potential error in velocity is largest when motion is computed with short image separations. Failing to correct a 10 cm (1 std dev. of IBE) height difference leads to a $\sim$85 m a^{-1} error when using data from the ERS tandem mission (1 day separation), whereas the error is only $\sim$2 m a^{-1} using successive 35 day repeat ERS or 24 day repeat RADARSAT passes. However, even with the longer repeat periods, errors of 10 m a^{-1} could occur in the worst case (e.g. if the true timing of a frontal passage was slightly different from the atmospheric-pressure model used to generate the IBE corrections).

In satellite altimetry time series, the relevance of the uncorrected IBE signal can be illustrated by using the 2 year Halley Base record of P_{air} as a test of height trends measured by the 35 day repeat of the ERS radar altimeter. About 20 height estimates will be obtained in this 2 year period. By choosing the time of the first ERS pass in this time interval at random through the first 100 days of P_{air} data and then taking a sample every 35 days, we obtain a histogram of the slope of the linear least-squares fit (Fig. 4). The mean trend is $\sim$4 cm a^{-1}, the same trend as in the original hourly time series of P_{air} at Halley. The standard deviation of the trend is $\sim$5 cm a^{-1}. It is possible to obtain apparent trends in ice surface height exceeding 15 cm a^{-1} (averaged over 2 years) simply due to ignoring true trends in P_{air} and undersampling the IBE in satellite-derived time series of η_{ice}.

The preceding analysis of altimetry presents an extreme example of trend errors due to satellite undersampling. The long-term trend in η_{ice} will be better defined with the $\sim$10 years of ERS altimetry that are now available. Errors
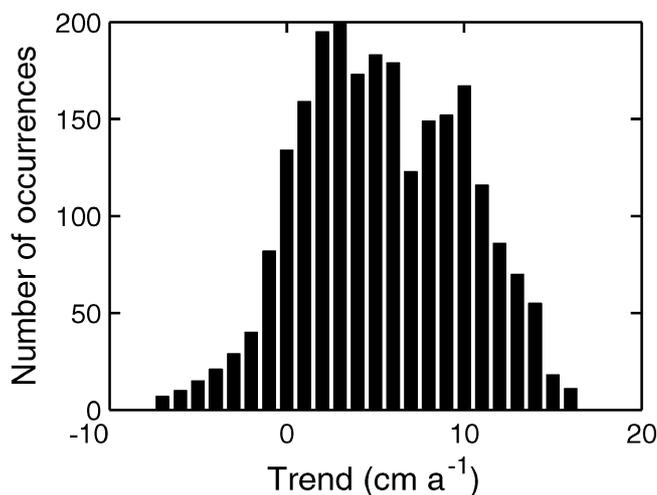

Fig. 4. Histogram of 2 year trend in ice-shelf surface elevation (cm a^{-1}) based on 35 day sampling of the 2 years of Halley air-pressure data used in this study. The mean trend is $\sim$4 cm a^{-1}, and the standard deviation is $\sim$5 cm a^{-1}. See text for methodology used to derive this figure.

will be reduced at crossovers where twice as many data are collected, and analyses can also take into account the generally large spatial scale of IBE corrections and the temporal offsets of adjacent ground tracks, which imply that combining altimetry from multiple nearby crossovers will reduce the standard deviation of the trend estimates. Nevertheless, as the analysis of the Halley time series of P_{air} shows, there can be trends of a few cm a^{-1} in η_{ice} associated with real trends in P_{air} on time-scales of 1–3 years. These time-scales are of interest, for example, when assessing ice-thickness changes associated with El Niño–Southern Oscillation (ENSO; Kwok and Comiso, 2002) and the Antarctic Circumpolar Wave (ACW; White and Peterson, 1996). We note also that future altimetry missions, such as the Geoscience Laser Altimeter System (GLAS) on the Ice, Cloud and land Elevation Satellite (ICESat), may have shorter mission lives and less frequent sampling at each crossover location than ERS, and thus have potential for larger errors in trend estimates if no correction for $\eta_{ice}(P_{air})$ is applied.

The inclusion of the ideal IBE in "tidal" corrections to η_{ice} reduces the weather-band variance of ice-shelf height to $\sigma^2(\eta'_{WB}) \sim 10$ cm^2. Further improvements in prediction of the response function $\eta_{ice}(P_{air})$ could be made by following Ponte and others (1991) and Ponte (1993), i.e. numerical modeling of SSH response to realistic atmospheric forcing. Such studies could include SSH response to various non-IBE processes such as shelf waves and wind-forced set-up near coasts. However, $\sigma^2 (\eta_{WB})$ is much less than the error variance associated with present-generation models of tides around Antarctica ($\sim$50–100 cm^2), so priority in effort should be directed towards improving the quality of tide models.

ACKNOWLEDGEMENTS

REFERENCES

Chelton, D. B. and D. B. Enfield. 1986. Ocean signals in tide gauge records. *J. Geophys. Res.*, **91**(B9), 9081–9098.

Doake, C. S. M. and 6 others. 2002. Tide-induced lateral movement of Brunt Ice Shelf, Antarctica. *Geophys. Res. Lett.*, **29**(8). (10.1029/2001GL014606.)

Foreman, M. G. G. 1977. *Manual for tidal heights analysis and prediction.* Patricia Bay, Victoria, B.C., Department of the Environment. Institute of Ocean Scneices. (Pacific Marine Science Report 77-10.)

Fricker, H. A. and L. Padman. 2002. Tides on Filchner–Ronne Ice Shelf from ERS radar altimetry. *Geophys. Res. Lett.*, **29**(12). (10.1029/2001GL014175.)

Gill, A. E. 1982. *Atmosphere–ocean dynamics.* San Diego, Academic Press. (International Geophysics Series 30.)

Goring, D. G. and A. Pyne. 2003. Observations of sea-level variability in Ross Sea, Antarctica. *NZ J. Marine Freshwater Res.*, **37**, 241–249.

King, M. and S. Aoki. 2002. Tidal observations on floating ice using a single GPS receiver. *Geophys. Res. Lett.*, **30**(3), 1138. (10.1029/2002GL016182.)

Kwok, R. and J. C. Comiso. 2002. Southern Ocean climate and sea ice anomalies associated with the Southern Oscillation. *J. Climate*, **15**(5), 487–501.

Padman, L., S. Erofeeva and I. Joughin. 2003. Tides of the Ross Sea and Ross Ice Shelf. *Antarct. Sci.*, **15**(01), 31–40.

Padman, L., H. A. Fricker, R. Coleman, S. Howard and L. Erofeeva. 2002. A new tide model for the Antarctic ice shelves and seas. *Ann. Glaciol.*, **34**, 247–254.

Pawlowicz, R., B. Beardsley and S. Lentz. 2002. Classical tidal harmonic analysis including error estimates in MATLAB using TTIDE. *Computers Geosci.*, **28**(8), 929–937.

Ponte, R. M. 1993. Variability in a homogeneous global ocean forced by barometric pressure. *Dyn. Atmos. Oceans*, **18**(3–4), 209–234.

Ponte, R. M., D. A. Salstein and R. D. Rosen. 1991. Sea-level response to pressure forcing in a barotropic numerical-model. *J. Phys. Oceanogr.*, **21**(7), 1043–1057.

Potter, J. R., J. G. Paren and M. Pedley. 1985. Tidal behaviour under an Antarctic ice shelf. *Br. Antarct. Surv. Bull.*, **68**, 1–18.

Ray, R. D. and B. V. Sanchez. 1989. *Radial deformation of the earth by oceanic tidal loading.* Goddard Space Flight Center. (NASA Technical memo. 100743.)

Rignot, E. and D. R. MacAyeal. 1998. Ice-shelf dynamics near the front of Filchner–Ronne Ice Shelf, Antarctica, revealed by SAR interferometry. *J. Glaciol.*, **44**(147), 405–418.

Rignot, E., L. Padman, D. R. MacAyeal and M. Schmeltz. 2000. Observation of ocean tides below the Filchner and Ronne Ice Shelves, Antarctica, using synthetic aperture radar: comparison with tide model predictions. *J. Geophys. Res.*, **105**(C8), 19,615–19,630.

White W. B. and R. Peterson. 1996. An Antarctic Circumpolar Wave in surface pressure, wind, temperature and sea ice extent. *Nature*, **380**(6576), 699–702.

Zumberge, J. F., M. B. Heflin, D. C. Jefferson, M. M. Watkins and F. H. Webb. 1997. Precise point positioning for the efficient and robust analysis of GPS data from large networks. *J. Geophys. Res.*, **102**(B3), 5005–5017.